Chapter 5
Co-electrohydrodynamic Forming of Biomimetic Polymer Materials for Diffusion Magnetic Resonance Imaging

Feng-Lei Zhou and Geoff J. M. Parker

Abstract Magnetic resonance imaging (MRI) is routinely used as a medical imaging modality in the disease detection, monitoring, and therapy response assessment in neurology and cancer. An attractive feature of MRI is its ability to provide non-invasive quantitative measurements relating to the tissue microenvironment. In MRI, a technique known as diffusion MRI can provide non-invasive quantitative information that is reflective of the microstructure of tissues, ranging from measurements of axonal packing in the brain, through measurements of myocardial fiber orientation in the heart to measurements of tumor cell size. These measurements are powerful, but they are not commonly used clinically, in part due to a lack of validation. Synthetic tissues, with known microstructural properties, provide one approach to providing such validation. This chapter presents how co-electrohydrodynamic (co-EHD) forming of polymer materials can be used to create synthetic tissues (or phantoms) for diffusion MRI by mimicking the cellular structure of tissues in the brain, heart, and tumor. Two types of co-EHD polymeric structures, i.e. hollow microfibres and microspheres, will be discussed with the focus on the shell and core materials and the relevant processes used. Three types of tissue-mimicking phantoms and their performance in pre-clinical or clinical MRI measurements will be highlighted.

Keywords Diffusion MRI · Co-electrohydrodynamics forming · Phantoms · Tissue-mimicking

F.-L. Zhou (✉) · G. J. M. Parker
Department of Medical Physics and Biomedical Engineering, University College London, London, UK
e-mail: fenglei.zhou@ucl.ac.uk

G. J. M. Parker
e-mail: geoff.parker@ucl.ac.uk

F.-L. Zhou
School of Pharmacy, University College London, London, UK

G. J. M. Parker
Bioxydyn Limited, Manchester, UK

© The Author(s), under exclusive license to Springer Nature Switzerland AG 2022
A. Vaseashta and N. Bölgen (eds.), *Electrospun Nanofibers*,
https://doi.org/10.1007/978-3-030-99958-2_5

5.1 Introduction

Magnetic resonance imaging (MRI) is routinely used as a medical imaging modality in the diagnosis of a wide range of diseases. Part of the attraction of MRI is its ability to provide non-invasive quantitative measurements relating to the tissue microenvironment. In particular, a technique known as diffusion MRI is able to provide non-invasive quantitative information that is reflective of the microstructure of tissues, ranging from measurements of axonal packing in the brain to measurements of tumor cell size. These measurements are powerful, but they are not commonly used clinically, in part due to a lack of validation. Synthetic tissues, with known microstructural properties, provide one approach to providing such validation. Here we discuss how co-electrohydrodynamic forming of polymer materials can be used to create test objects (or phantoms) for diffusion MRI by mimicking the cellular structure of tissues.

5.2 Co-electrohydrodynamic Forming of Hollow Polymeric Materials

Hollow polymeric nano/microstructures with cylindrical or spherical geometries are of special interest for use in encapsulation, controlled release, filtration, and nanoreactors, which currently are mainly fabricated using hard-templating, soft-templating, and self-templating synthesis [1]. However, those templating strategies often require multiple steps due to extra procedures to remove the template/core materials. Co-electrohydrodynamic (co-EHD) forming was firstly demonstrated by Loscertales et al. in 2002 [2] to fabricate core–shell structured water–oil nanoparticles, and then in 2004 was extended by the same researchers to produce hollow polymeric nano/microfibres (later called co-electrospinning, Fig. 5.1a) [2] and nano/microspheres (later called co-electrospraying, Fig. 5.1b) [3]. The main advantage of co-electrospinning/spraying lies in the fact that they are one-step processes and allow flexibility of controlling the sizes (i.e. wall thickness, inner diameters) and patterning of hollow fibers and spheres.

5.2.1 Co-electrospinning of Hollow Polymeric Fibres

Co-electrospinning (or coaxial electrospinning) has greatly expanded the versatility of electrospinning by enabling core–shell structured or hollow fibre fabrication, providing multi-functional/structural properties from a single fibre. By forming a fibre that consists of two or more complementary materials in the core and the shell, one can design complex fibres with a combination of properties that are not achieved in homogeneous nanofibres from single-nozzle electrospinning.

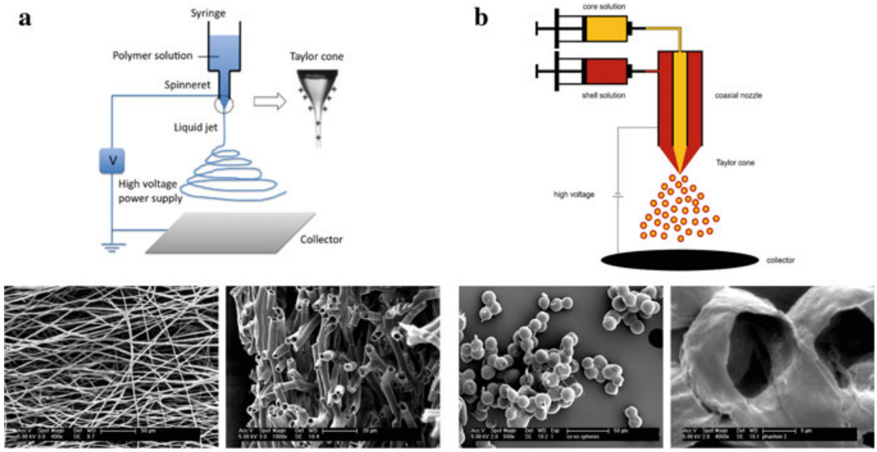

Fig. 5.1 Co-EHD forming of hollow polymeric materials. **a** Schematic of co-electrospinning (reproduced from [4], an open access journal published under a CC BY-NC-SA 3.0 license.) and SEM micrographs of morphology and cross-section of co-electrospun hollow microfibres; **b** schematic of co-electrospraying (reproduced from [5] with permission, copyright Elsevier) and SEM micrographs of morphology and cross-section of co-electrosprayed hollow microspheres

Co-electrospinning was firstly combined with sol–gel chemistry to produce tetraethylorthosilicate (TEOS) hollow nanofibres in one step from non-polymer core–shell combination [2]. In several following studies, Zussman et al. [6] extended this technique to different polymer solutions (e.g. poly (ε-caprolactone) (PCL) shell and poly(ethylene oxide) (PEO) core). The rapid solidification of shell solution and the evaporation of core solution through the shell was proposed to be responsible for one-step formation of hollow microfibres in coaxial electrospinning [6, 7]. The size and morphology of resultant co-electrospun fibres were closely affected by core/shell materials properties (e.g. solvent and concentration), process parameters (e.g. solution flow rate, electric field) [8]. Since then this field has been growing rapidly and extensively, as evidenced by two review articles published by Moghe et al. [9] in 2008 and Han et al. [10] in 2019, in which early history and current status, basic theories, process parameters of co-electrospinning and various applications of co-electrospun fibres were critically summarised.

Biomedical applications frequently using co-electrospun fibres, primary in tissue scaffolds, wound dressings and drug delivery, have been, and continue to be, vigorously investigated, resulting in promising advances and novel approaches. For instance, one of the most exciting developments in coaxial electrospinning is high-throughput production of hollow nanofibres by using a needleless coaxial slit spinneret [11].

Precise deposition of core–shell structured or hollow microfibres in coaxial electrospinning on a desired location or specific pattern is also an area of current progress. The concept of direct-writing co-electrospinning was firstly demonstrated by Zhou et al. [12]. Dramatically reducing the gap (often called working distance) between the nozzle and the collector to a few millimetres suppressed the instability of the fluid jet. By using such a jet with a motor-controlled X–Y stage collector, position-controlled deposition of patterned fibres was realized, as shown in Fig. 5.2a. By utilizing a rotating collector (Fig. 5.2b) in direct writing co-electrospinning using

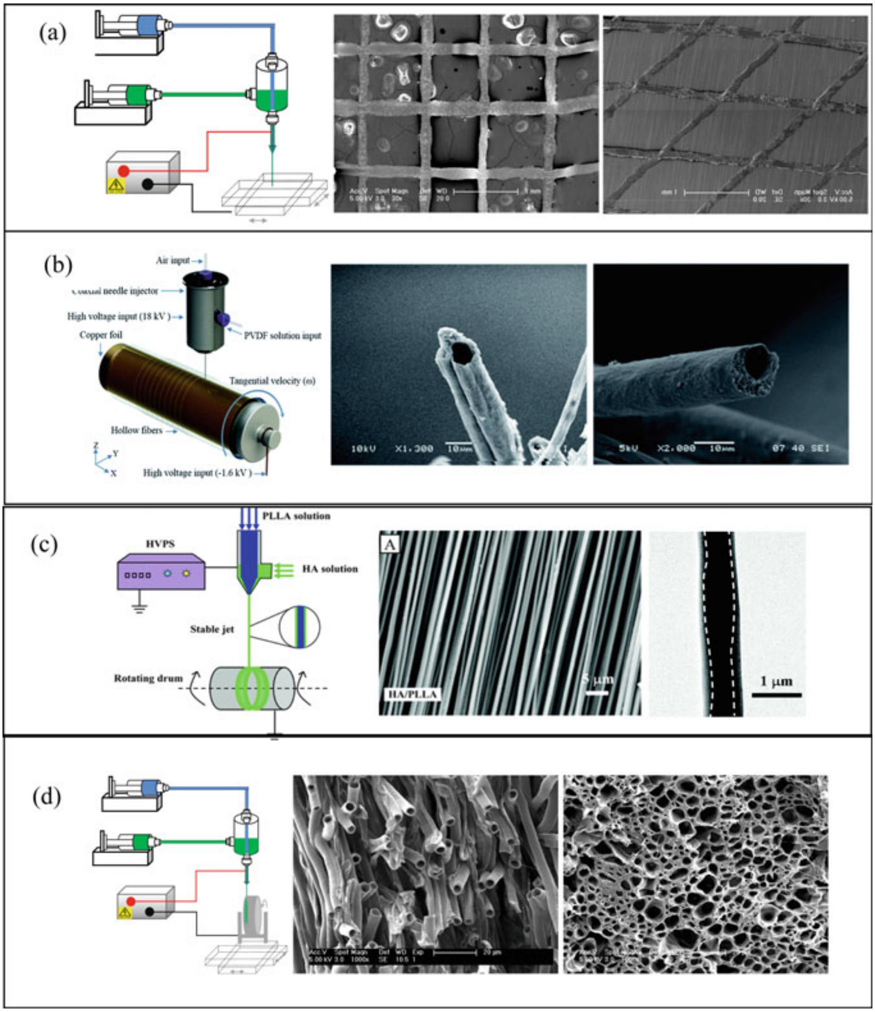

Fig. 5.2 Direct writing of core–shell structured or hollow polymeric fibres: **a** near-field coaxial electrospinning of patterned sugar-PCL core-sheath fibres (reproduced from [12] with permission, copyright Elsevier); **b** near-field coaxial electrospinning of hollow PVDF fibres (reproduced from [13] with the permission from the Royal Society of Chemistry); **c** far-field coaxial electrospinning of PLA-PEO shell and HA core (reproduced from [15] with the permission from the Royal Society of Chemistry); **d** far-field coaxial electrospinning of PCL shell and PEO core (reproduced from [16], an open access article published by Elsevier under a CC-BY license)

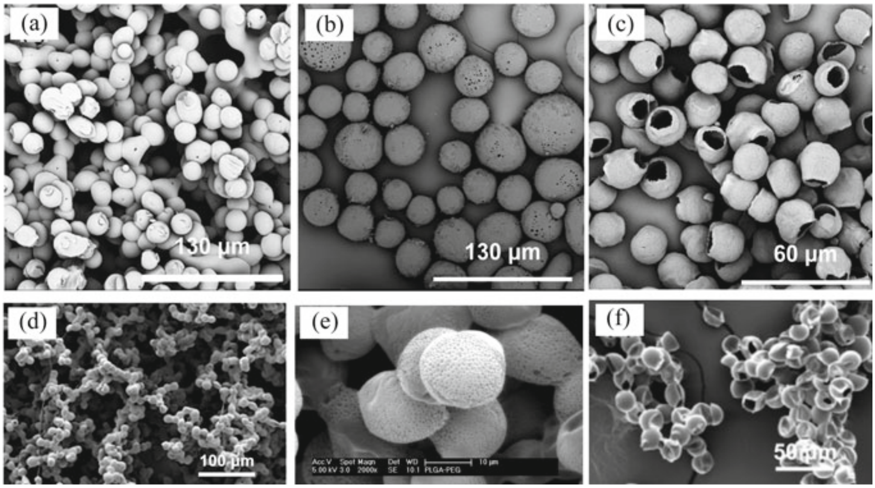

Fig. 5.3 Co-electrosprayed hollow polymeric microspheres with (**a**, **d**) solid surface, (**b**, **e**) porous surface, and (**e**, **f**) single surface opening, from PCL (**a**–**c**) (reproduced from [18], an open access article published by Elsevier under a CC-BY license) and PLGA (**d**–**f**) polymers [(**d**) and (**f**) were reproduced from [19], an open access article published by Elsevier under a CC-BY license]

an 1 mm working distance, well-defined hollow piezoelectric polyvinylidene fluoride (PVDF) fibres with tuneable inner diameters were fabricated [13]. At a working distance of 10 cm, a direct coaxial jet was still observed, which allowed the formation of well-defined and highly aligned hollow poly(d,l-lactic-co-glycolic acid) (PLGA) fibres from PLGA-PEO shell-core solution [14]. The addition of ultra-high molecular weight PEO (Mw > 5 M Da) into a poly(L-lactic acid) (PLA) shell solution helped maintain the state of the direct jet even when the working distance was further increased to 30 cm in the coaxial electrospinning using hyaluronic acid (HA) core solution (Fig. 5.2c) [15]. Zhou et al. further combined a rotating drum with an X–Y stage (Fig. 5.2d) to collect hollow PCL microfibres with variable fibre orientation/packing [16]. In particular, the gap between those hollow fibres could be tuned by varying the translation speed of the X–Y stage [16].

5.2.2 *Coaxial Electrospraying of Hollow Polymer Particles*

The studies of coaxial electrospraying can be divided into two categories. The first category is focused on developing biodegradable polymeric particles encapsulating biological agents for specific imaging and therapeutic applications. PCL and PLGA are two FDA-approved synthetic polymers having good biocompatibility and biodegradability, and are most commonly used materials in coaxial electrospraying of core–shell spherical particles for biomedical applications [17]. Co-electrospraying has been employed to fabricate hollow polymeric particles with various surface microstructural characteristics, including solid surface, porous surface and with a single surface opening (Fig. 5.3). These are made from PCL and PLGA by varying factors including core/shell solution combinations, process parameters (e.g. flow rate) and/or collecting media [18, 19]. Furthermore, it has been shown that the ratio of shell thickness to radius of core–shell microspheres can also be adjusted by varying these factors [20].

The second coaxial electrospraying category includes theoretical studies focusing on computational and numerical simulations. The development of commercial software for computational fluid dynamics (CFD), including FLUENT 15.0 software (ANSYS), has encouraged the simulation of cone-jet behaviour and core–shell droplet formation from miscible shell/core solution combinations in single [21] and double-nozzle co-electrospraying [22]. More recently, a complete axisymmetric model of coaxial electrospraying under constant electrical permittivities and conductivities, and strict immiscibility of shell/core liquids was presented [23]. It can be envisaged that these computational and numerical simulations could greatly benefit the optimization of the co-electrospraying process.

5.3 Tissue Microstructure Mimicking Phantoms for Diffusion MRI

5.3.1 Brain, Heart and Tumour Microstructure

Axons in white matter create a highly anisotropic fibrous tissue. Myelinated axons are elliptic or circular in cross section, with diameters ranging from 0.16 and up to 9 μm [24] (Fig. 5.4a). Myocardial tissue (heart muscle) also consists of highly anisotropic fibrous tissues characterised by an array of interconnecting fibres with a radius of 21.4 ± 16.8 μm [25], as evidenced by longitudinal histology (Fig. 5.4b).

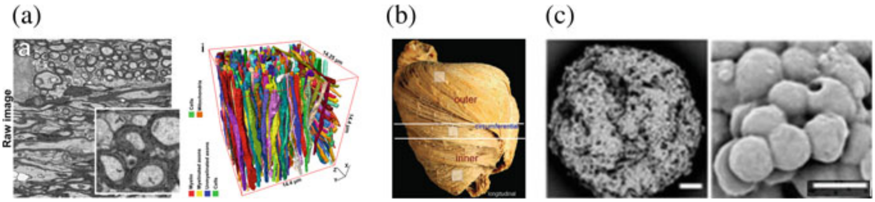

Fig. 5.4 Tissue microstructure in brain, heart and tumour: **a** 2D (left) SEM micrograph and simulation (right) showing axon size and axonal orientation in rat brain (reproduced from [24], an open access article published by Springer Nature under a CC-BY license); **b** a digital photograph showing a dissection (right) revealing the progression of the helical angle in porcine heart (reproduced from [26] with the permission from the BMJ Publishing Group Ltd.); **c** SEM micrographs of human pancreatic cancer cells (KP4) (reproduced from [27], an open access article published by Springer Nature under a CC-BY license). Scale bars in **c** are 50 μm (left) and 10 μm (right)

From the outer, through the middle to the outer layer in myocardium muscle there is a gradual and relatively even progression of helical angulation, from 'left-handed' through 'horizontal' to 'right-handed' orientation [26]. The microstructural properties (Fig. 5.4c) in solid tumour are often described in terms of cell size, which typically range from 10 to 20 μm [27], with intra- and extracellular packing density/volume fraction showing large variations. In each setting, the microstructural characteristics of tissue may vary with disease, and therefore represent an attractive target for diagnosis and monitoring of therapeutic interventions.

Diffusion MRI provides the ability to infer the microstructure of tissues by monitoring the diffusion of water molecules within and between cells; changes in cellularity affect water diffusion, and therefore macroscopically-recorded diffusion MRI signals. There have been an increasing number of studies on probing changes in tissue microstructure via diffusion MRI, not only as a diagnostic marker of diseases but also as a measure of treatment response to various therapies. There is increasing demand for diffusion MRI validation due to the exponential growth of the field of microstructural imaging [28].

5.3.2 Co-EHD Microstructural Phantoms for Diffusion MRI

The term "phantom" is used here for well-characterized test objects in terms of size and composition that can be used for evaluating the accuracy and precision of MRI methods to study tissue microstructure (for recent reviews of phantoms for quantitative MRI in general see [29, 30], respectively). The majority of microstructural phantoms currently in existence are used to provide a gold standard for the validation of MRI methods probing brain microstructure, although interest is growing in the development and application of such phantoms for validating microstructure measurements in tumours and in the heart.

Brain Tissue-Mimicking Phantom

As shown in Fig. 5.5a, co-electrospinning of uniaxially aligned hollow microfibres was achieved using a rotating drum fixed on an X–Y translation stage, resulting in fibres deposited in strip form; fibre strips were then characterised via SEM & μ-CT for ground truth, and finally packed as ~10–15 fibre layers into a MR visible liquid-filled test tube to form a phantom. Diffusion MRI measurement of these brain tissue mimicking phantoms has demonstrated that: (1) as shown in Fig. 5.5b, fractional anisotropy (FA—a composite diffusion MRI measurement of microscopic fibre orientation coherence and micro-geometric anisotropy) decreases linearly with an increase in the mean inner diameter of the fibres, whereas the radial diffusivity was shown to increase (indicating, as expected, that molecular diffusion across the section of the fibres is greater when the diameter of the section is larger) [31]; (2) fibre tractography results match the fibre orientations present in the white and grey matter phantoms (Fig. 5.5c) [32]; (3) diffusion MRI results for the phantoms show

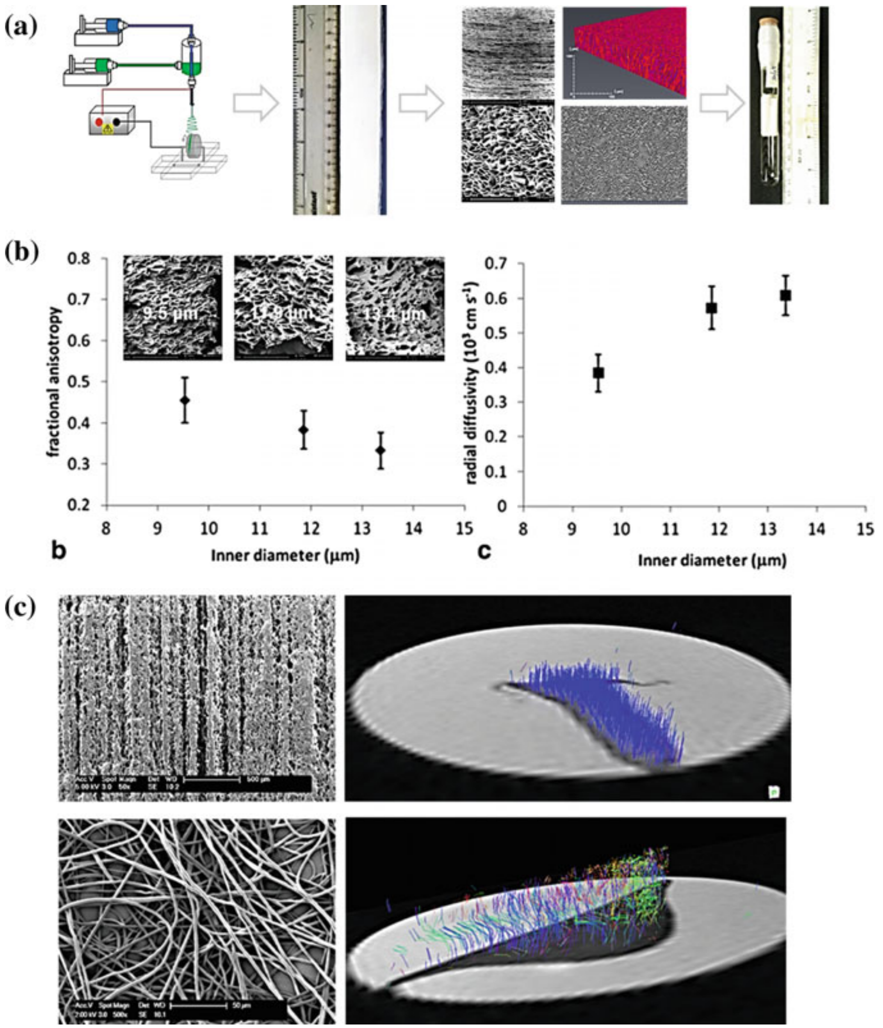

Fig. 5.5 Brain-mimicking fibre phantoms and their MRI performance: **a** flowchart of co-electrospinning of brain white matter phantom (reproduced from [34] with the permission from Springer, Cham); **b** effects of fibre size (reproduced from [31], an open access article published by John Wiley and Sons under a CC-BY license) and **c** fibre orientation (reproduced from [32] with permission form IEEE) in brain phantom on MR measurement (i.e., mean diffusivity and FA values); **d** repeatability over time of ADC and FA values on diffusion time of brain phantoms (reproduced from [33], an open access article published by John Wiley and Sons under a CC-BY license)

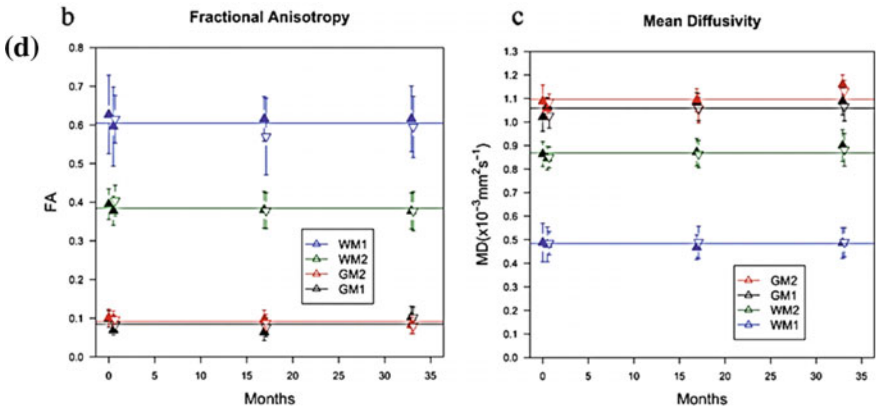

Fig. 5.5 (continued)

low variability for measured mean diffusivity and FA over a period of 33 months, indicating good material stability (Fig. 5.5d) [33].

Cardiac Tissue-Mimicking Phantom

Cardiac diffusion MRI can measure microstructural changes in the size and distribution of myocardial fibres, but despite recent developments, is not yet used for clinical management. The use of physiologically relevant phantoms helps the development of new imaging methods such as this by providing validation of the proposed measurements. However, the majority of current microstructure phantoms are for diffusion MRI in brain. They are also generally simplistic and lacking important features present in the myocardium, such as the helical arrangement of myocardial fibred. To address this, Teh et al. used three layers of co-electrospun hollow microfibres, wound at different helix angles, to design and construct the first-of-its-kind left-ventricular myocardium mimicking phantom (Fig. 5.6a) [35]. The values of apparent diffusion coefficient (ADC) and FA acquired from this phantom were found to be physiologically relevant and stable for a testing period of 4 months (a longer study was not conducted) (Fig. 5.6b). Importantly, the co-electrospun cardiac phantom had fibres orientations similar to those present in the left ventricle (Fig. 5.6c), suggesting that this phantom could act as a valuable tool for development and validation of new techniques for cardiac microstructure via diffusion MRI and for quality assurance in longitudinal and multicentre studies.

Tumor Cell-Mimicking Phantom

Diffusion MRI is considered as a useful tool to study solid tumours. However, the interpretation of the diffusion MRI signal and validation of quantitative measurements has to date proved challenging, due in part to the lack of a standard reference material that can mimic tumour cell microstructure. Zhou and McHugh et al. [19] showed that co-electrosprayed hollow PLGA microspheres can be used to mimic tumour cells mimicking materials and to construct a new generation of diffusion

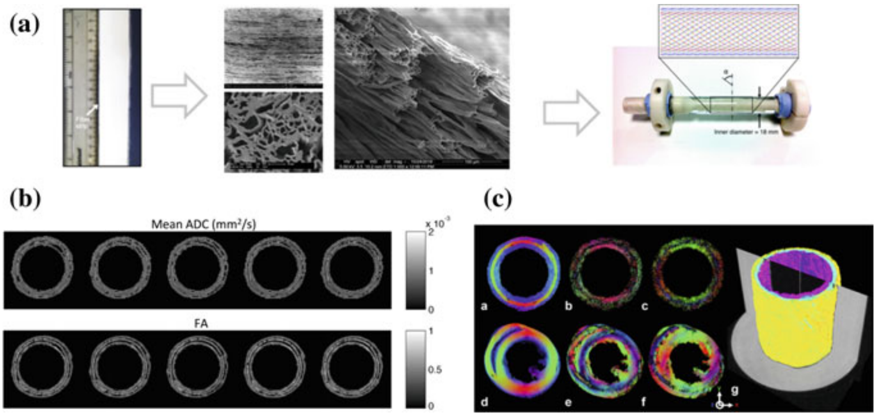

Fig. 5.6 Cardiac-mimicking fibre phantom and its MRI performance (reproduced from [35], an open access article published by John Wiley and Sons under a CC-BY license): **a** flowchart of co-electrospinning of cardiac phantom; **b** ADC and FA maps of cardiac phantom acquired over time; **c** fibre orientation transition in the phantom (top) and rat heart for comparison (bottom) and 3D fibre tractography (right) in the cardiac phantom

MRI phantom (Fig. 5.7a) [36]. The ADC values of the phantom were found to be dependent on the diffusion time, indicating that the phantom reflects the interaction of diffusing molecules with the cell-mimicking structure (Fig. 5.7b), and vary little over the test period of 42 weeks (Fig. 5.7c) [36]. These results provide evidence that co-electrosprayed hollow PLGA microspheres can restrict/hinder water diffusion as cells do in tumour tissue, implying that co-electrosprayed phantom may be suitable for use as a quantitative validation and calibration tool for diffusion MRI of cancer.

5.4 Summary

Diffusion MRI is a powerful non-invasive method for quantifying elements of tissue microstructure, with a range of diagnostic applications. Co-electrohydrodynamic forming of polymer materials has proven to be an effective approach to create tissue mimicking materials that allow this powerful medical imaging technique to be validated, allowing greater confidence in the technique and moving it a step closer to widespread clinical use.

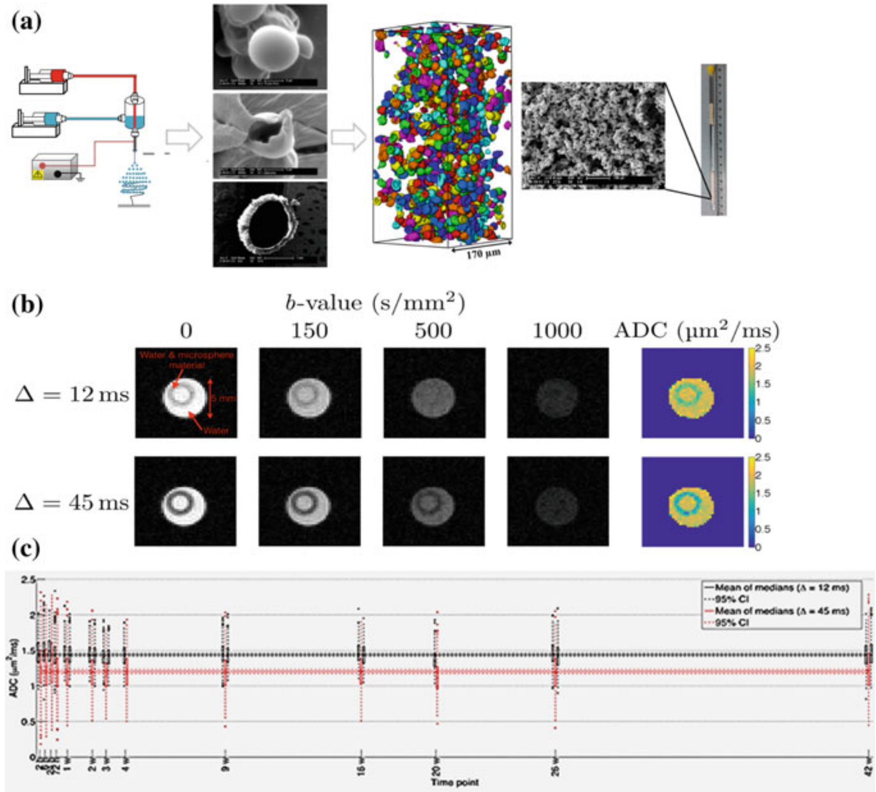

Fig. 5.7 Tumour cell-mimicking sphere phantom and its MRI performance: **a** flowchart of co-electrospraying of tumour cell phantom (reproduced from [19] with permission, copyright Elsevier)); **b** ADC maps acquired at two settings of diffusion time [36] and **c** the corresponding ADC values over 42 weeks reproduced from [36], an open access article published by John Wiley and Sons under a CC-BY license)

Acknowledgements This research was supported by NIHR UCLH Biomedical Research Centre (BRC) grant, and UK-MRC ImagingBioPro grant (MR/R025673/1), and UCL Department of Medical Physics and Biomedical Engineering and EPSRC (EP/M020533/1; CMIC Pump-Priming Award). GJM Parker has a shareholding and part time appointment and directorship at Bioxydyn Ltd. which provides MRI services. He is also a director and shareholder of Queen Square Analytics Ltd, which provides quantitative MRI services.

References

1. Wang, X., et al. (2016). Synthesis, properties, and applications of hollow micro-/nanostructures. *Chemical Reviews, 116*(18), 10983–11060.
2. Loscertales, I. G., et al. (2004). Electrically forced coaxial nanojets for one-step hollow nanofiber design. *Journal of the American Chemical Society, 126*(17), 5376–5377.
3. Loscertales, I. G., et al. (2002). Micro/nano encapsulation via electrified coaxial liquid jets. *Science, 295*(5560), 1695–1698.
4. Li, F., Song, Y., & Zhao, Y. (2010). Core-shell nanofibers: Nano channel and capsule by coaxial electrospinning. In A. Kumar (Ed.), *Nanofibres*. Intechopen.
5. Smeets, A., et al. (2020). Gastro-resistant encapsulation of amorphous solid dispersions containing darunavir by coaxial electrospraying. *International Journal of Pharmaceutics, 574*, 118885.
6. Dror, Y., et al. (2007). One-step production of polymeric microtubes by co-electrospinning. *Small (Weinheim an der Bergstrasse, Germany), 3*(6), 1064–1073.
7. Arinstein, A., & Zussman, E. (2007). Postprocesses in tubular electrospun nanofibers. *Physical Review E, 76*(5), 056303.
8. Halaui, R., et al. (2011). Development of micro-scale hollow fiber ultrafiltration membranes. *Journal of Membrane Science, 379*(1), 370–377.
9. Moghe, A. K., & Gupta, B. S. (2008). Co-axial electrospinning for nanofiber structures: Preparation and applications. *Polymer Reviews, 48*(2), 353–377.
10. Han, D., & Steckl, A. J. (2019). Coaxial electrospinning formation of complex polymer fibers and their applications. *ChemPlusChem, 84*(10), 1453–1497.
11. Yan, X., et al. (2015). Slit-surface electrospinning: A novel process developed for high-throughput fabrication of core-sheath fibers. *PLoS ONE, 10*(5), e0125407.
12. Zhou, F.-L., et al. (2011). Jet deposition in near-field electrospinning of patterned polycaprolactone and sugar-polycaprolactone core–shell fibres. *Polymer, 52*(16), 3603–3610.
13. Pan, C.-T., et al. (2015). Near-field electrospinning enhances the energy harvesting of hollow PVDF piezoelectric fibers. *RSC Advances, 5*(103), 85073–85081.
14. Sitt, A., et al. (2016). Microscale rockets and picoliter containers engineered from electrospun polymeric microtubes. *Small (Weinheim an der Bergstrasse, Germany), 12*(11), 1432–1439.
15. Yuan, H., et al. (2016). Highly aligned core–shell structured nanofibers for promoting phenotypic expression of vSMCs for vascular regeneration. *Nanoscale, 8*(36), 16307–16322.
16. Zhou, F.-L., et al. (2015). Production and cross-sectional characterization of aligned co-electrospun hollow microfibrous bulk assemblies. *Materials Characterization, 109*, 25–35.
17. Zhang, L., et al. (2012). Coaxial electrospray of microparticles and nanoparticles for biomedical applications. *Expert Review of Medical Devices, 9*(6), 595–612.
18. Zhou, F.-L., et al. (2017). Hollow polycaprolactone microspheres with/without a single surface hole by co-electrospraying. *Langmuir, 33*(46), 13262–13271.
19. Zhou, F.-L., et al. (2019). Co-electrospraying of tumour cell mimicking hollow polymeric microspheres for diffusion magnetic resonance imaging. *Materials Science and Engineering: C, 101*, 217–227.
20. Gao, Y., et al. (2016). Optimising the shell thickness-to-radius ratio for the fabrication of oil-encapsulated polymeric microspheres. *Chemical Engineering Journal, 284*, 963–971.
21. Yan, W.-C., et al. (2016). Computational study of core-shell droplet formation in coaxial electrohydrodynamic atomization process. *AIChE Journal, 62*(12), 4259–4276.
22. Yan, W.-C., Tong, Y. W., & Wang, C.-H. (2017). Coaxial electrohydrodynamic atomization toward large scale production of core-shell structured microparticles. *AIChE Journal, 63*(12), 5303–5319.
23. López-Herrera, J. M., et al. (2020). A numerical simulation of coaxial electrosprays. *Journal of Fluid Mechanics, 885*, A15.
24. Abdollahzadeh, A., et al. (2019). Automated 3D axonal morphometry of white matter. *Scientific Reports, 9*(1), 6084.

25. Wang, B., et al. (2012). Structural and biomechanical characterizations of porcine myocardial extracellular matrix. *Journal of Materials Science: Materials in Medicine*, *23*(8), 1835–1847.
26. Partridge, J. B., et al. (2014). Linking left ventricular function and mural architecture: What does the clinician need to know? *Heart, 100*(16), 1289.
27. Minami, F., et al. (2021). Morphofunctional analysis of human pancreatic cancer cell lines in 2- and 3-dimensional cultures. *Scientific Reports, 11*(1), 6775.
28. Novikov, D. S., et al. (2019). Quantifying brain microstructure with diffusion MRI: Theory and parameter estimation. *NMR in Biomedicine, 32*(4), e3998.
29. Keenan, K. E., et al. (2018). Quantitative magnetic resonance imaging phantoms: A review and the need for a system phantom. *Magnetic Resonance in Medicine, 79*(1), 48–61.
30. Fieremans, E., & Lee, H.-H. (2018). Physical and numerical phantoms for the validation of brain microstructural MRI: A cookbook. *NeuroImage, 182*, 39–61.
31. Hubbard, P. L., et al. (2015). Biomimetic phantom for the validation of diffusion magnetic resonance imaging. *Magnetic Resonance in Medicine, 73*(1), 299–305.
32. Ye, A. Q., et al. (2014). Diffusion tensor MRI phantom exhibits anomalous diffusion. In *2014 36th Annual International Conference of the IEEE Engineering in Medicine and Biology Society*.
33. Grech-Sollars, M., et al. (2018). Stability and reproducibility of co-electrospun brain-mimicking phantoms for quality assurance of diffusion MRI sequences. *NeuroImage, 181*, 395–402.
34. Zhou, F.-L., et al. (2015). Co-electrospun brain mimetic hollow microfibres for diffusion magnetic resonance imaging. In A. Macagnano, E. Zampetti, & E. Kny (Eds.), *Electrospinning for high performance sensors* (pp. 289–304). Springer International Publishing.
35. Teh, I., et al. (2016). Biomimetic phantom for cardiac diffusion MRI. *Journal of Magnetic Resonance Imaging, 43*(3), 594–600.
36. McHugh, D. J., et al. (2018). A biomimetic tumor tissue phantom for validating diffusion-weighted MRI measurements. *Magnetic Resonance in Medicine, 80*(1), 147–158.

Feng-Lei Zhou obtained the B.S. degree in textile engineering and the M.S. degree in textile materials from Qingdao University (China) and the Ph.D. degree in textiles from the University of Manchester (UK). He is a Senior Research Fellow at UCL, working in the Centre for Medical Image Computing and School of Pharmacy. From 2010 to 2019, he worked as a Research Associate and then a Research Fellow in the Manchester Centre for Imaging Sciences. He has general research interests in electrohydrodynamic (EHD) processing and polymer materials. In the past decade, he has participated in several cross-disciplinary research projects funded by the EU FP7, EPSRC and CRUK, in which he pioneered the development of tissue-mimicking phantoms for the validation of diffusion MRI in neurology, cancer, and heart. He has inspired and gathered together a circle of key collaborators with fruitful outputs from 10+ world-leading imaging centers in the UK, EU, USA and China. More recently his research has expanded to EHD 3D printing of dielectric elastomer actuators, MRI guided theranostic materials, and smart wearables. Dr. Zhou has published 46 articles in peer-reviewed journals and one edited book chapter in the book "Electrospinning for High-Performance Sensor", which is one of the most downloaded books of the last five years on the Springer website. He is a member of the Fiber Society (USA) and the Aerosol Society (UK).

Geoff J. M. Parker graduated with a B.Sc. degree in physics from the University of Manchester before completing his Ph.D. on dynamic contrast-enhanced MRI in cancer at the Institute of Cancer Research in London. He then moved to the NMR Research Unit at the Institute of Neurology, UCL, where he worked on a range of MRI techniques, including relaxation time measurement methods, brain atrophy measurements, and diffusion MRI tractography methods, which he applied to multiple sclerosis and epilepsy. In 2001 he moved to the Department of Imaging Science and Biomedical Engineering at the University of Manchester, where he continued to develop and apply quantitative MRI methods in a range of conditions, including cancer, neurology, and lung disease. Starting as a research fellow, he gained promotion to full professor in 2007. He moved to take up his current position—Professor of Healthcare Engineering, Imaging and Enterprise within UCL's Centre for Medical Image Computing (CMIC)—in 2019. His research group continues to work on quantitative MRI, including the development of tissue-mimicking phantom materials for diffusion MRI. In addition to his academic work, he founded Bioxydyn in 2009 to translate quantitative MRI methods into healthcare, and he continues to be the Chief Executive Officer of the company. In 2020 he co-founded Queen Square Analytics, which is pioneering the use of machine learning methods applied to MRI to help diagnose and treat neurological diseases. Prof. Parker is Deputy Editor for Magnetic Resonance in Medicine (MRM), Editorial Board member of BMC Medicine, Senior Fellow of the International Society for Magnetic Resonance in Medicine (ISMRM), Member of the ISMRM Board of Trustees, past Secretary and Treasurer of the British Chapter ISMRM, Deputy Director of the UCL Institute of Healthcare Engineering, and is a member of the EPSRC Peer Review College.